

## Research in Astronomy and Astrophysics

---

### PAPER

# Flaring activity from quiescent states in neutron-star X-ray binaries

To cite this article: Dimitris M. Christodoulou *et al* 2018 *Res. Astron. Astrophys.* **18** 142

View the [article online](#) for updates and enhancements.

## Flaring activity from quiescent states in neutron-star X-ray binaries

Dimitris M. Christodoulou<sup>1,2</sup>, Silas G. T. Laycock<sup>1,3</sup>, Demosthenes Kazanas<sup>4</sup> and Ioannis Contopoulos<sup>5,6</sup>

<sup>1</sup> Lowell Center for Space Science and Technology, University of Massachusetts Lowell, Lowell, MA, 01854, USA

<sup>2</sup> Dept. of Mathematical Sciences, Univ. of Massachusetts Lowell, Lowell, MA, 01854, USA;  
[dimitris\\_christodoulou@uml.edu](mailto:dimitris_christodoulou@uml.edu)

<sup>3</sup> Dept. of Physics & Applied Physics, Univ. of Massachusetts Lowell, Lowell, MA, 01854, USA;  
[silas\\_laycock@uml.edu](mailto:silas_laycock@uml.edu)

<sup>4</sup> NASA/GSFC, Laboratory for High-Energy Astrophysics, Code 663, Greenbelt, MD 20771, USA;  
[demos.kazanas@nasa.gov](mailto:demos.kazanas@nasa.gov)

<sup>5</sup> Research Center for Astronomy and Applied Mathematics, Academy of Athens, Athens 11527, Greece;  
[icontop@academyofathens.gr](mailto:icontop@academyofathens.gr)

<sup>6</sup> National Research Nuclear University, Moscow 115409, Russia

Received 2018 May 1; accepted 2018 June 13

**Abstract** We examine systematically the observed X-ray luminosity jumps (or flares) from quiescent states in millisecond binary pulsars (MSBPs) and high-mass X-ray binary pulsars (HMXBPs). We rely on the published X-ray light curves of seven pulsars: four HMXBPs, two MSBPs and the ultraluminous X-ray pulsar M82 X-2. We discuss the physics of their flaring activities or lack thereof, paying special attention to their emission properties when they are found on the propeller line, inside the Corbet gap or near the light-cylinder barrier. We provide guiding principles for future interpretations of faint X-ray observations, as well as a method of constraining the propeller lines and the dipolar surface magnetic fields of pulsars using a variety of quiescent states. In the process, we clarify some disturbing inaccuracies that have made their way into the published literature.

**Key words:** accretion — accretion disks — pulsars: individual (4U 0115+63, V 0332+53, M82 X-2, Aquila X-1, SAX J1808.4–3658, AX J0049.4–7323, 1A 0535+262) — stars: magnetic fields — stars: neutron — X-rays: binaries

### 1 INTRODUCTION

X-ray observations over the past 25 years have produced a wealth of information about X-ray binary pulsars, both those that occur in high-mass X-ray binaries (HMXBPs) and millisecond binary pulsars (MSBPs) (for reviews, see Phinney & Kulkarni 1994; Lorimer 2008; Reig 2011; Papitto et al. 2014; Campana & Di Salvo 2018). But theory has not made analogous progress, mainly because of the many complexities involved in the accretion process. To date, observers have tried to make sense of their results by using the fundamental results of Ghosh & Lamb (Ghosh et al. 1977; Ghosh & Lamb 1979), but determinations of magnetospheric radii, pulsar magnetic fields and disk accretion torques are still highly uncertain to

say the least (Wang 1987, 1995, 1996; Chakrabarty et al. 1997; Bildsten et al. 1997; Frank et al. 2002). In this paper, we describe how a pulsar magnetosphere is expected to evolve in X-ray binaries when they are found in low-power and quiescent states (Papitto & Torres 2015), without using the above uncertain quantities for guidance. The only exception is the surface magnetic field  $B$  in cases in which it is known from detections of *multiple* resonant scattering features (cyclotron absorption lines) in the X-ray spectra.

We interpret the X-ray light curves of HMXBPs and MSBPs in a consistent manner by determining the threshold luminosities of low-power states exclusively from the observations. Three such thresholds exist: the propeller line (Illarionov & Sunyaev 1975; Stella et al.

1986; Christodoulou et al. 2016) that is relevant for all accreting binaries; the lower boundary of the Corbet (1996) gap that is relevant for all HMXBs and for MSBPs with weak surface magnetic fields; and the light-cylinder barrier (Campana et al. 1998) that is relevant only for MSBPs with strong magnetic fields (say,  $B \sim 10^8$  G). The applicable thresholds for each pulsar class are illustrated in Figure 1.

These three states can be discerned from observations because the pulsars should exhibit different behaviors: On the propeller line, the pulsars are expected to show intense variability only if  $B$  is strong enough (say,  $B \sim 1$  TG) to push against the inflowing disk matter. On the lower boundary of the Corbet gap, the pulsars are expected to undergo recurrent flares that should appear as minor luminosity bursts that may or may not reach the propeller line, depending on changes in the inflow rate of the disk matter. No such eruptions are expected from the quiescent state at the light cylinder. The reason is that MSBPs whose magnetospheres have expanded out to the light cylinder possess sufficiently strong magnetic fields that cannot be pushed around by the inflowing disk matter for as long as the mass flow rate remains small.

At this point, we must clarify the terminology and definitions that we use for the various emission states and thresholds in order to avoid confusion with the many disparate terms used in the literature (references are given in the following paragraph): (a) The propeller line is not a “propeller state” and it does not belong to the so-called “propeller regime;” it is the state of minimum accretion that occurs when the inner edge of the disk corotates with the magnetospheric boundary. (b) All states with X-ray luminosities lower than that of the propeller line are “non-accreting propeller states” and they belong to the “propeller regime.” However, they come in two varieties, those states in which flaring activities place them inside the Corbet gap and the states with even lower luminosities that fall well below the bottom of the gap and occur only in MSBPs with strong magnetic fields. (c) Because of this distinction between non-accreting states, we avoid using the imprecise terms in quotation marks above and we refer instead to the specific thresholds on or near which the various states occur.

We use as examples the published X-ray light curves of seven pulsars:

- (a) Four HMXBPs, 4U 0115+63 (Tsygankov et al. 2016a; Wijnands & Degenaar 2016; Rouco Escorial et al. 2017), V 0332+53 (Tsygankov et al. 2016a; Wijnands & Degenaar 2016; Vybornov et al.

- 2018), AX J0049.4–7323 (Ducci et al. 2018) and 1A 0535+262 (Doroshenko et al. 2014);
- (b) two MSBPs, Aquila X-1 (Campana et al. 1998; Ootes et al. 2018) and SAX J1808.4–3658 (Campana et al. 2008; Sanna et al. 2017);
- (c) and the ultraluminous X-ray (ULX) pulsar M82 X-2 (Bachetti et al. 2014; Tsygankov et al. 2016b; Brightman et al. 2016; Dall’Osso et al. 2016).

Our results can guide searches for propeller-line emission and for fainter states in X-ray pulsars with varying spin periods ( $\sim 1$  ms – 1 ks) (Christodoulou et al. 2016, 2017b) as well as in neutron-star ULX sources (Earnshaw et al. 2018).

In Section 2, we provide the theoretical framework for understanding faint X-ray emission from MSBPs and HMXBPs. In Section 3, we interpret the flaring activities of the seven pulsars in our sample when they occupy low-power or quiescent states and, where possible, we calculate their  $B$  values. Some of the magnetic fields have been previously determined from observed resonant scattering features in the spectra, and then a direct comparison can readily be made. In Section 4, we summarize our conclusions.

## 2 THEORETICAL CONSIDERATIONS

For faint HMXBPs (Fig. 1a), two luminosity thresholds are important: the propeller-line luminosity  $L_{\text{prop}}$  (Illarionov & Sunyaev 1975; Stella et al. 1986) at the state of minimum accretion and the gap luminosity  $L_{\text{gap}}$  (Corbet 1996; Campana 1997) for magnetospheric emission from the bottom of the Corbet gap. For faint MSBPs with strong magnetic fields (Fig. 1b), a third threshold may also become important, the luminosity for weak magnetospheric emission  $L_{\text{lc}}$  from the radius of the light cylinder (Campana et al. 1995). All three luminosity thresholds have been briefly summarized by Campana et al. (1998). Here we define these quantities using the customary cgs units and canonical pulsar parameters (mass  $M = 1.4 M_{\odot}$  and radius  $R = 10$  km).

The state of minimum accretion (the propeller line) occurs when the magnetospheric radius has expanded out to the corotation radius

$$R_{\text{co}} = 1.68 \times 10^8 \left( \frac{P_S}{1 \text{ s}} \right)^{2/3} \text{ cm}, \quad (1)$$

where  $P_S$  is the spin period of the pulsar. The radius of the light cylinder is given by

$$R_{\text{lc}} \equiv \frac{c P_S}{2\pi} = 4.77 \times 10^9 \left( \frac{P_S}{1 \text{ s}} \right) \text{ cm}, \quad (2)$$

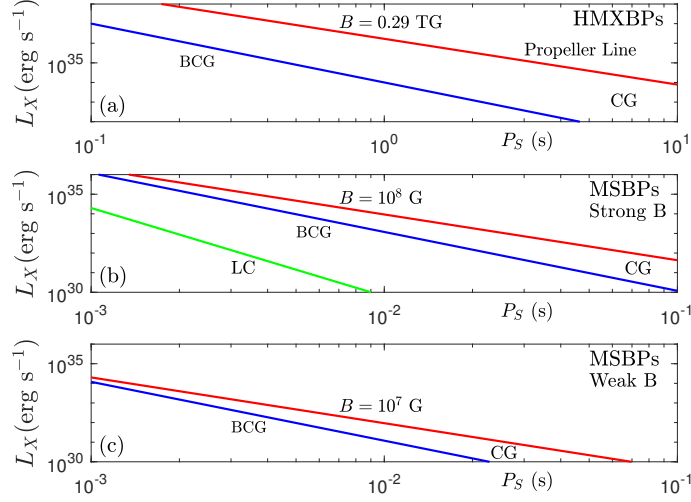


**Fig. 1** Relevant X-ray luminosity thresholds versus spin period for HMXBPs and for MSBPs. The propeller lines are drawn for the given magnetic-field values. The area of the Corbet gap is denoted by CG, the bottom of the gap by BCG and the light-cylinder threshold by LC (the latter is relevant only for MSBPs with strong magnetic fields). The slopes of the lines, from top to bottom, are  $-7/3$  (Eq. (3)),  $-3$  (Eq. (6)) and  $-9/2$  (Eq. (7)).

where  $c$  is the speed of light. The ratio  $R_{lc}/R_{co} = 28.4$  for  $P_S = 1$  s, but it decreases to just 2.84 for  $P_S = 1$  ms. Furthermore, for all MSBPs of interest, the light cylinder always lies outside corotation: the requirement that  $R_{lc} \leq R_{co}$  is satisfied only for spin periods of  $P_S \leq 43 \mu\text{s}$ . On the other hand, the bottom of the Corbet gap is also characterized by an effective radius which lies between the other two radii for all cases of interest.

An estimate of the propeller-line luminosity was given by Stella et al. (1986) who assumed that the magnetospheric radius coincides with the corotation radius at the state of minimum accretion, viz.

$$L_{\text{prop}} = 2.0 \times 10^{37} \left( \frac{B}{1 \text{ TG}} \right)^2 \left( \frac{P_S}{1 \text{ s}} \right)^{-7/3} \text{ erg s}^{-1}, \quad (3)$$

where  $B$  is the dipolar surface magnetic field defined by the equation

$$\mu \equiv BR^3, \quad (4)$$

and  $\mu$  is the magnetic moment of the dipole. The bottom of the Corbet (1996) gap lies below  $L_{\text{prop}}$  by a factor of  $1/\Gamma$ , where

$$\Gamma = 168 \left( \frac{P_S}{1 \text{ s}} \right)^{2/3}, \quad (5)$$

that is  $L_{\text{gap}} = L_{\text{prop}}/\Gamma$  or, equivalently,

$$L_{\text{gap}} = 1.2 \times 10^{35} \left( \frac{B}{1 \text{ TG}} \right)^2 \left( \frac{P_S}{1 \text{ s}} \right)^{-3} \text{ erg s}^{-1}. \quad (6)$$

Finally, an approximation for the magnetospheric luminosity at the light-cylinder radius was obtained by

Campana et al. (1998) who estimated the mass inflow rate at that radius, viz.

$$L_{lc} = 6.3 \times 10^{28} \left( \frac{B}{1 \text{ TG}} \right)^2 \left( \frac{P_S}{1 \text{ s}} \right)^{-9/2} \text{ erg s}^{-1}. \quad (7)$$

The requirement that  $L_{\text{gap}} \leq L_{lc}$  is satisfied only for spin periods of  $P_S \leq 65 \mu\text{s}$ , whereas  $L_{\text{gap}} \geq L_{\text{prop}}$  is satisfied only for  $P_S \leq 465 \mu\text{s}$ . These nonrestrictive conditions lead to a systematic order of the X-ray luminosity thresholds, viz.

$$L_{lc} < L_{\text{gap}} < L_{\text{prop}},$$

for all pulsars with spin periods  $P_S > 465 \mu\text{s}$ .

Analogous to  $\Gamma$ , we also define the ratio  $\Delta \equiv L_{\text{gap}}/L_{lc}$ , viz.

$$\Delta = 1.90 \times 10^6 \left( \frac{P_S}{1 \text{ s}} \right)^{3/2}. \quad (8)$$

For the entire range of spin periods 1 ms–1 ks,  $\Delta \gg \Gamma$ , thus the bottom of the Corbet gap always lies a lot closer to the propeller-line luminosity than the light-cylinder luminosity.

For HMXBPs, the light cylinder does not provide a level of quiescent magnetospheric emission because  $R_{lc} \gg R_{co}$ , but the bottom of the Corbet gap does just that. Observations of this quiescent state ( $L_{\text{gap}}$ ) provide an unambiguous determination of the surface magnetic fields using Equation (6). For MSBPs with relatively strong magnetic fields ( $B \sim 10^8$  G), magnetospheric pressure is sufficiently strong and it can push out

and reach  $R_{lc}$ , in which case observations of this quiescent state ( $L_{lc}$ ) provide an unambiguous determination of their surface magnetic fields using Equation (7). We provide observed examples of both types of quiescent states in Section 3 below.

### 3 X-RAY LIGHT CURVES OF SELECTED PULSARS

In what follows, we meta-analyze the published light curves of the seven pulsars listed in Section 1. Also, where possible, we calculate their surface magnetic fields using the identified quiescent states and we compare the results to previously published determinations. All observed and calculated quantities are summarized in Table 1.

#### 3.1 Guiding Principles

Our analysis relies on the following guiding principles (see also Fig. 1):

- (a) *Inside the Corbet gap.*—X-ray emission can occur from the upper half and from the lower half of the Corbet gap, but the emission mechanisms differ. Nevertheless, the gap is expected to be washed out considerably in all X-ray sources (a fact known to Corbet 1996, but not to many others who treated it as an absolute gap; see, e.g., Sections 3.2 and 3.3 below):
- (i) In the upper half, the pulsar has crossed below the propeller line but it continues to accrete weakly because the magnetic field lines behind the centrifugal barrier are still loaded with matter that descends toward the pulsar and some minor leakage may still occur at higher latitudes (Spruit & Taam 1993; Doroshenko et al. 2014). This view is also supported by the results of Christodoulou et al. (2016) that clearly show 10 Magellanic Be/X-ray pulsars emitting just below the propeller line in faint states where no pulsations have ever been measured and the spectra are always soft. Consequently, the propeller line cannot be identified unambiguously in observations of individual pulsars by any abrupt drops in X-ray flux, as has been attempted in the past.
  - (ii) In the lower half, X-ray emission can be detected as a result of flaring that originates from the bottom of the Corbet gap. As we detail below, some flares are strong enough to reach up into the upper half of the gap and, upon recurrence of accretion, to the propeller line.
- (b) *Quiescent HMXBPs.*—HMXBPs with relatively strong magnetic fields (say,  $B \sim 1$  TG) in quiescence at the bottom of the Corbet gap can be reactivated by the inward push of inflowing matter that momentarily pushes the magnetosphere back toward corotation. This produces flaring activity that exhibits luminosity jumps falling well within the gap. As a result, the bottom of the gap can be identified by observations and then the propeller line can be determined from  $L_{prop} = \Gamma L_{gap}$ . No knowledge of the magnetic field is required in this procedure. In the past, the opposite procedure has been attempted and it has produced erroneous results because the propeller line was empirically chosen to be much lower than where it really lies (Sections 3.2 and 3.3 below). On the other hand, HMXBPs with weak magnetic fields are not expected to reach the bottom of the Corbet gap, so any flares, if they happen at all, should occur near/above the propeller line.
- (c) *High State of Quiescent MSBPs.*—MSBPs with relatively weak magnetic fields (say,  $B \lesssim 10^7$  G) will also reside at the bottom of the Corbet gap in quiescence. They are also subject to flaring activity (the magnetosphere gets pushed around by changes in the inflow rate), and their propeller lines can also be determined from  $L_{prop} = \Gamma L_{gap}$  with no input from the magnetic field.
- (d) *Low State of Quiescent MSBPs.*—MSBPs with relatively strong magnetic fields (say,  $B \gtrsim 10^8$  G) will not reside at the bottom of the Corbet gap in quiescence. Instead, their magnetospheres are sufficiently strong to push out to the radius of the light cylinder, where no push back can be expected from the minor accumulation of matter, so no flaring activity is expected to develop. In this case, the two higher luminosity thresholds can be determined from  $L_{gap} = \Delta L_{lc}$  and  $L_{prop} = \Gamma \Delta L_{lc}$ .

In the above cases where either  $L_{gap}$  or  $L_{lc}$  can unambiguously be identified as the lowest quiescent state, the dipolar surface magnetic field can readily be determined from Equation (6) or Equation (7), respectively (see Table 1).

#### 3.2 4U 0115+63

Following a giant type II outburst in 2015, the source luminosity decreased to quiescent levels where it did



**Table 1** HMXBPs and MSBPs: X-ray Observations and Calculated Results

No.	Pulsar ID	$P_S$ (s)	$L_{1c}$ ( $\text{erg s}^{-1}$ )	$L_{\text{gap}}$ ( $\text{erg s}^{-1}$ )	$L_{\text{prop}}$ ( $\text{erg s}^{-1}$ )	$B$ (G)
HMXBPs						
1	4U 0115+63	3.61		$4.5 \times 10^{33}$	$\longrightarrow$ $1.8 \times 10^{36}$	$\longrightarrow$ $1.3 \times 10^{12}$
2	V 0332+53	4.376		$1.5 \times 10^{34}$	$\longrightarrow$ $6.7 \times 10^{36}$	$\longrightarrow$ $3.2 \times 10^{12}$
3	AX J0049.4–7323	750		$2.5 \times 10^{27}$	$\longleftarrow$ $3.5 \times 10^{31}$	$\longleftarrow$ $3.0 \times 10^{12}$
4	1A 0535+262	103.3		$2.7 \times 10^{30}$	$\longleftarrow$ $1.0 \times 10^{34}$	$\longleftarrow$ $5.0 \times 10^{12}$
MSBPs						
5	Aquila X-1	$1.8 \times 10^{-3}$	$1.0 \times 10^{33}$	$\longrightarrow$ $1.5 \times 10^{35}$	$\longrightarrow$ $3.6 \times 10^{35}$	$\longrightarrow$ $8.4 \times 10^7$
6	SAX J1808.4–3658	$2.5 \times 10^{-3}$	$8.4 \times 10^{29}$	$\longleftarrow$ $2.0 \times 10^{32}$	$\longrightarrow$ $6.0 \times 10^{32}$	$\longrightarrow$ $5.0 \times 10^6$
ULX Pulsar						
7	M82 X-2	1.37		$7.7 \times 10^{33}$	$\longleftarrow$ $1.6 \times 10^{36}$	$\longrightarrow$ $4.1 \times 10^{11}$

Notes: Arrows show the flow of the calculations and, in all cases, they point to calculated quantities. For M82 X-2, anisotropic X-ray luminosities are listed, reduced by a beaming factor of  $b = 111$  (Christodoulou et al. 2017a).

not remain flat (Tsygankov et al. 2016a; Wijnands & Degenaar 2016; Rouco Escorial et al. 2017). Several minor outbursts occurred aperiodically and a few stronger outbursts were detected as the source was crossing periastron; they were all interpreted as metastable states of magnetospheric emission from inside the Corbet gap. Tsygankov et al. (2016a) used an abrupt drop in the 0.5–10 keV luminosity to identify empirically the propeller line at  $7 \times 10^{35} \text{ erg s}^{-1}$ . Their identification can be shown to be incorrect: for  $P_S = 3.61 \text{ s}$ , Equations (5) and (3) produce the wrong values of the gap threshold ( $1.8 \times 10^{33} \text{ erg s}^{-1}$ , lower than the observed value of  $L_{\text{gap}} \approx (4 - 5) \times 10^{33} \text{ erg s}^{-1}$ ) and the magnetic field (0.8 TG), respectively. The magnetic field is known from the presence of 11.5 keV and 23 keV cyclotron lines in the spectrum (White et al. 1983). Using  $E_{\text{cyc}} = 11.5 \text{ keV}$  as the fundamental energy ( $n = 1$ ) and the canonical value of the gravitational redshift  $z_g = 0.306$ , we find from the equation

$$B = \frac{1 + z_g}{n} \left( \frac{E_{\text{cyc}}}{11.57 \text{ keV}} \right) \quad (9)$$

that  $B = 1.3 \text{ TG}$ .

From the observations of Tsygankov et al. (2016a), we adopt  $L_{\text{gap}} = 4.5 \times 10^{33} \text{ erg s}^{-1}$ , in which case we find that  $L_{\text{prop}} = 1.8 \times 10^{36} \text{ erg s}^{-1}$  and  $B = 1.3 \text{ TG}$ , in agreement with the value from Equation (9). This value of  $L_{\text{prop}}$  shows that the source had crossed below the propeller line while still radiating for a few more days before it dropped abruptly to the lower boundary of the Corbet gap.

### 3.3 V 0332+53

Following its own giant type II outburst in 2015, the source luminosity decreased to quiescent levels

where it showed very similar evolution as 4U 0115+63 (Tsygankov et al. 2016a; Wijnands & Degenaar 2016; Vybornov et al. 2018). Tsygankov et al. (2016a) used an abrupt drop in the 0.5–10 keV luminosity to identify empirically the propeller line at  $1 \times 10^{36} \text{ erg s}^{-1}$ . Their identification is likely incorrect: for  $P_S = 4.376 \text{ s}$ , Equation (3) produces the wrong value of the magnetic field (1.25 TG). The magnetic field is believed to be known from the presence of a single 28.5 keV cyclotron line in the spectrum (Makishima et al. 1990; Vybornov et al. 2018). Using  $E_{\text{cyc}} = 28.5 \text{ keV}$  as the fundamental energy ( $n = 1$ ) and  $z_g = 0.306$  in Equation (9), we find that  $B = 3.2 \text{ TG}$ .

The luminosities in the lower gap are flaring even when the source is not near periastron but still shows distinct bursts into the Corbet gap (Tsygankov et al. 2016a; Wijnands & Degenaar 2016). This makes it hard to determine the level of  $L_{\text{gap}}$ . We adopt a value of  $L_{\text{gap}} = 1.5 \times 10^{34} \text{ erg s}^{-1}$  which lies near the top of the flares. This may seem a factor of  $\sim 4$  higher than the average value of the flares, but it is necessary in order to reproduce the correct value of the magnetic field. In this case, we find that  $L_{\text{prop}} = 6.7 \times 10^{36} \text{ erg s}^{-1}$  and  $B = 3.2 \text{ TG}$ .

We note here an alternative possibility that uses the observed average of the gap luminosities  $L_{\text{gap},2} = 4 \times 10^{33} \text{ erg s}^{-1}$ . Then we find that  $L_{\text{prop},2} = 1.8 \times 10^{36} \text{ erg s}^{-1}$  and  $B_2 = 1.7 \text{ TG}$ . These values are close to the determinations of Tsygankov et al. (2016a) and they could be correct if the observed cyclotron line is not the fundamental but the first harmonic. Using  $n = 2$ ,  $E_{\text{cyc}} = 28.5 \text{ keV}$  and  $z_g = 0.306$  in Equation (9), we then find that  $B = 1.6 \text{ TG}$ . In such case, V 0332+53 would not only have a similar light curve as 4U 0115+63, but the two sources would also have comparable magnetic fields, thus they would be twins.

Irrespective of which of the above two scenarios is correct, the light curve shows that the source was radiating for a few more days after it had crossed below the propeller line. This is seen most clearly in figure 2 of Tsygankov et al. (2016a).

### 3.4 AX J0049.4–7323

This 750 s pulsar in the Large Magellanic Cloud has shown intense variability over a period of 17 years and it was monitored by virtually all X-ray telescopes (Ducci et al. 2018). Its 0.3–8 keV X-ray luminosity has varied from  $1.6 \times 10^{37} \text{ erg s}^{-1}$  down to  $8.0 \times 10^{33} \text{ erg s}^{-1}$ .

It is included in our sample as a typical example of a very long period HMXBP for which the three luminosity thresholds cannot be mapped out with current capabilities, even though the pulsar may have a strong magnetic field. Ducci et al. (2018) estimated that  $B = 3 \text{ TG}$ . For this value and for  $P_S = 750 \text{ s}$ , we find from Equation (3) that  $L_{\text{prop}} = 3.5 \times 10^{31} \text{ erg s}^{-1}$  and  $L_{\text{gap}} = 2.5 \times 10^{27} \text{ erg s}^{-1}$ .

Therefore, the intense variability seen over the past 17 years occurs well above the propeller line by factors of 230 or higher. The minor outbursts seen in this case can be easily distinguished from the flaring activities of shorter-period pulsars which occur at the bottom of the Corber gap: these minor bursts do not originate from a luminosity plateau that would effectively define  $L_{\text{prop}}$  for AX J0049.4–7323.

### 3.5 1A 0535+262

The spectrum of this  $P_S = 103.3 \text{ s}$  pulsar exhibits a cyclotron line at  $E_{\text{cyc}} = 46 \text{ keV}$  and its first harmonic near  $\sim 100 \text{ keV}$ , so its magnetic field is estimated to be  $B = 5 \text{ TG}$  (Naik et al. 2008; Caballero et al. 2013). Using these values in Equation (3) and Equation (6), we find that

$$L_{\text{prop}} = 1.0 \times 10^{34} \text{ erg s}^{-1},$$

and that  $L_{\text{gap}} = 2.7 \times 10^{30} \text{ erg s}^{-1}$ . Thus, the source cannot be observed at the bottom of the Corbet gap and its flaring activity reported by Doroshenko et al. (2014) occurs near/above the propeller line (not inside the gap, as these authors speculated): Doroshenko et al. (2014) observed a low-level outburst reaching a 0.2–4 keV luminosity of  $1.3 \times 10^{34} \text{ erg s}^{-1}$  and another *Suzaku* detection reported a 0.2–12 keV flux that was 6 times higher (Naik et al. 2008).

Thus, this source has exhibited normal variability above the propeller line and there is no mystery about

how it could continue to accrete (cf., Doroshenko et al. 2014). It is also understood why all of the above observations of these faint states managed to measure highly significant pulsations for this source. The results of Christodoulou et al. (2016) on Magellanic pulsars show that highly significant pulsations were measured in about half of the sources that were found to reside on the lowest Magellanic propeller line.

The variability observed in 1A 0535+262 is quite interesting and other long-period HMXBPs (say,  $P_S = 40 - 200 \text{ s}$ ) with strong magnetic fields should exhibit such generic behavior.<sup>1</sup> Conversely, detection of flares in long-period pulsars should indicate that (a) they occur above the propeller line, and (b) the sources possess strong surface magnetic fields. This is because such sources can be detected only above  $L_{\text{prop}}$ , where there is a continual tug of war by the inflowing matter trying to push back the strong pulsar magnetosphere.

### 3.6 Aquila X-1

This source is a prime example of an MSBP ( $P_S = 1.8 \text{ ms}$ ) with strong magnetic field that exhibits all three important X-ray luminosity thresholds (Sect. 2) during its low-power evolution and subsequent progress toward quiescence (fig. 1a in Campana et al. 1998; Ootes et al. 2018).

After its 1997 outburst, Aquila X-1 evolved toward quiescence within 30 days past its maximum luminosity (Campana et al. 1998). In the process, it crossed the propeller line  $L_{\text{prop}}$ , dropped down to the bottom of the Corbet gap  $L_{\text{gap}}$  and continued on to quiescence which occurred at the luminosity of the light-cylinder barrier  $L_{\text{lc}}$ . The drop from the propeller line to the light-cylinder barrier took less than 10 days. In the light-cylinder state, the source showed no sign of flaring for at least the next 20 days. This is understood to be a consequence of its strong magnetic field. Matter pile-up on to the magnetosphere is minimal and incapable of pushing back against the strong magnetospheric pressure.

We ascertained from figure 1a of Campana et al. (1998) that

$$L_{\text{lc}} = 1 \times 10^{33} \text{ erg s}^{-1}$$

<sup>1</sup> Indeed, the recent investigation of faint states in EXO 2030+375 (Fürst et al. 2017) shows that the lowest luminosity was detected by *Swift* ( $L_{\text{min}} = 1.0 \times 10^{34} \text{ erg s}^{-1}$ ) and that the X-ray spectrum became much softer at that faint level. For this 42 s pulsar,  $B = 1.24 \text{ TG}$  has been obtained from a sequence of cyclotron lines with fundamental  $E_{\text{cyc}}(n = 1) \approx 11 \text{ keV}$ . These values imply that  $L_{\text{prop}} = 5.0 \times 10^{33} \text{ erg s}^{-1}$ , just below  $L_{\text{min}}$ . As in 1A 0535+262 and AX J0049.4–7323, the observed variability occurs above the propeller line and it is a generic feature.

in the 1.5–10 keV *BeppoSAX*/MECS band. For  $P_S = 1.8$  ms, Equations (8) and (5) give  $\Delta = 145$  and  $\Gamma = 2.5$ , respectively, implying that  $L_{\text{gap}} = 1.45 \times 10^{35} \text{ erg s}^{-1}$  and  $L_{\text{prop}} = 3.62 \times 10^{35} \text{ erg s}^{-1}$ , respectively. These values are lower than those determined by Campana et al. (1998) by a factor of 4, yet they fit the observed light curve well. They rely on the above identification of  $L_{1c}$ ; no other threshold from Campana et al. (1998) could be used because then the faintest observations would fall below the light-cylinder barrier (as is actually seen in fig. 1a of the original paper).

Any of the threshold luminosities can be used to estimate the surface magnetic field. We find that  $B = 8.4 \times 10^7$  G. If however one allows for the faintest observations to fall below the light-cylinder threshold (as in Campana et al. 1998), then  $B$  turns out to be larger by a factor of 2. Such a strong magnetic field appears to be responsible for the different evolutions of Aquila X-1 and SAX J1808.4–3658 (see below). The determined value falls at the bottom of the range of  $B$  values identified for Aquila X-1 by analyzing quasi-periodic oscillations assumed to originate at the inner edge of a Keplerian disk (but the assumption that the accretion disk is Keplerian is questionable all by itself).

### 3.7 SAX J1808.4–3658

This accreting millisecond pulsar ( $P_S = 2.5$  ms) was monitored by *Swift*/XRT (0.3–10 keV) during its 2005 outburst (Campana et al. 2008) and during its 2015 outburst (Sanna et al. 2017). Similar results were also reported by Hartman et al. (2008) and Patruno et al. (2009). Furthermore, many uncertain estimates of the magnetic field exist in the wide range of  $0.4\text{--}6 \times 10^8$  G. Campana et al. (2008) supported one of the lower values, viz.  $B = 7 \times 10^7$  G.

All observational campaigns revealed intense flaring activities after the spectacular outbursts had subsided. Some of the flares are quite strong and can be attributed to periastron passages, but other minor bursts are also present and quite frequent. This led Campana et al. (2008) to define two quiescent states past outburst: state A with an average luminosity of  $5 \times 10^{32} \text{ erg s}^{-1}$  and state B with an average luminosity of  $2 \times 10^{32} \text{ erg s}^{-1}$ . These two neighboring states are also visible in the Sanna et al. (2017) data, so they seem to be a generic feature at the faint end of the post-outburst evolution. Furthermore, unlike Aquila X-1, this source showed no sign of descending to the light-cylinder luminosity for

which Equation (8) predicts a value smaller than the faintest observations (state B) by a factor of  $\sim 240$ .

For this 2.5 ms pulsar, Equation (5) shows that  $L_{\text{prop}} = 3L_{\text{gap}}$  only, so an immediate interpretation of the two nearby states is that state A is the propeller line and state B occurs at the bottom of the Corbet gap. For  $L_{\text{gap}} = 2 \times 10^{32} \text{ erg s}^{-1}$ , Equation (6) gives

$$B = 5 \times 10^6 \text{ G in state B ,}$$

and a similar value is obtained for state A.

This value of  $B$  is an order of magnitude lower than the value in Campana et al. (2008), but it is not unreasonable given the host of uncertainties surrounding previous determinations. The low value of  $B = 5 \times 10^6$  G is supported by the fact that the source makes no attempt to expand toward the light cylinder: in MSBPs, accretion and pile-up of matter on to the magnetosphere at the bottom of the gap are weak and a strong magnetic field (e.g., the above-mentioned  $B = 7 \times 10^7$  G) should have been capable of pushing out all the way to the light-cylinder barrier, just as in the case of Aquila X-1. There is no sign of such evolution from state B in SAX J1808.4–3658, so its magnetic field is expected to be weak and certainly not as high as  $\sim 10^8$  G.

### 3.8 M82 X-2

After *NuSTAR* discovered pulsations from this ULX source (Bachetti et al. 2014), multiyear *Chandra* (0.5–10 keV) archival data were analyzed (Tsygankov et al. 2016b; Brightman et al. 2016) in order to determine the long-term evolution of this 1.37 s ULX pulsar. The observations showed that the source has repeatedly bounced between its bright ultraluminous state with an isotropic luminosity of  $L_{\text{max}} = 2 \times 10^{40} \text{ erg s}^{-1}$  and a low state with an isotropic luminosity of  $L_{\text{min}} = 1.7 \times 10^{38} \text{ erg s}^{-1}$ , comparable to the Eddington limit

$$L_{\text{Edd}} = 1.77 \times 10^{38} \text{ erg s}^{-1} .$$

Furthermore, Dall’Osso et al. (2016) obtained  $L_{\text{min}}$  as an upper limit of a null detection when the source was in deep quiescence. This extremely high value of  $L_{\text{min}}$  was interpreted by Tsygankov et al. (2016b) as the luminosity at the bottom of the Corbet gap and it produced what we believe is an unphysical value of the magnetic field ( $\sim 10^{14}$  G; Eq. (6)). The assumption that  $L_{\text{min}} = L_{\text{gap}}$  also implies an absurd propeller-line value of  $3.5 \times 10^{40} \text{ erg s}^{-1} > L_{\text{max}}$ , which this pulsar has never attained in 17 years of monitoring.



We include this ULX pulsar in our sample in order to demonstrate that it is not unusual in its low state; in fact it does not appear to be unusual in any state when emission is assumed to be anisotropic. Our interpretation of the bimodal evolution of M82 X-2 is that the source bounces between its high state during outbursts and the propeller line, thus we believe that it has never been detected inside the Corbet gap (Christodoulou et al. 2017a). Furthermore, we believe that its emission is beamed toward the observer. The beaming factor was determined to be  $b = L_{\max}/L_{\text{Edd}} = 111$  assuming that the true anisotropic luminosity during outbursts cannot exceed  $L_{\text{Edd}}$ . This assumption leads to a beamed propeller-line luminosity of  $L_{\text{prop}} = L_{\min}/b = 1.6 \times 10^{36} \text{ erg s}^{-1}$  and a modest value of the surface magnetic field ( $B = 0.41 \text{ TG}$ ). The other known ULX pretenders harboring neutron stars also have comparable values of  $B$ , which explains why they have never been observed below an isotropic luminosity of  $5 \times 10^{37} \text{ erg s}^{-1}$  (Christodoulou et al. 2017a).

For  $P_S = 1.37 \text{ s}$  in M82 X-2, then  $\Gamma = 207$  and using the above anisotropic value of  $L_{\text{prop}}$ , we find that  $L_{\text{gap}} = 7.7 \times 10^{33} \text{ erg s}^{-1}$  for the bottom of the Corbet gap and

$$b L_{\text{gap}} = 8.5 \times 10^{35} \text{ erg s}^{-1}$$

for the corresponding apparent isotropic gap luminosity. M82 X-2 has never been observed emitting at such an extremely low level. Furthermore, its jump factor of  $J = 2$  is above the lowest known Magellanic propeller line (Christodoulou et al. 2018). This value is completely independent of whether the source is beaming and it provides an indication as to the strength of  $B$  irrespective of the accretion regime. Such a small  $J$ -value implies that the low state of the pulsar lies slightly above the lowest Magellanic propeller line, which is characterized by a modest value of  $B = 0.29 \text{ TG}$  (Christodoulou et al. 2016); therefore, it supports the determined value of  $B = 0.41 \text{ TG}$  and the assumption of beamed emission.

Thus, it appears that M82 X-2 can barely descend to its propeller line and this can be explained naturally as the result of its relatively weak (sub-teragauss) magnetic field. It is extremely unlikely that such a weak magnetic field can overcome the ram pressure of the infalling gas and push the magnetospheric radius beyond corotation. It is also unlikely that the source can produce minor flaring activity just above the propeller line. Indeed, no such flares have been observed from M82 X-2. This not only argues in favor of a weak magnetic field—it also argues against identifying the low state with the bottom of the

Corbet gap: as we have seen in Sections 3.2 and 3.3, flaring activities from the gap luminosities are quite common in HMXBPs with magnetic fields of 1.3 TG or higher.

#### 4 SUMMARY AND CONCLUSIONS

Using the guiding principles of quiescent emission from HMXBPs and MSBPs that we laid out in Sections 2 and 3.1, we revisited the light curves of a sample of seven pulsars (Table 1) in the subsections of Section 3. A unifying theme of our analysis is that the mass inflow rate  $\dot{M}$  alone does not drive the evolution of X-ray binary pulsars in their faint and low-power states, as is commonly believed, because of the powerful influence of the inflowing accretion disk during outbursts. Instead, the magnetic field of the pulsar also determines to a large extent the evolution in and near low-power and quiescent states. (But these are the states in which  $\dot{M}$  is especially weak, so it could not possibly control the evolution of the pulsar all by itself.) For example, a strong magnetic field can push out to the location of the light cylinder in MSBPs, whereas a strong magnetic field can barely push out to the bottom of the Corbet (1996) gap in HMXBPs because the light cylinder is too far out in the disk and cannot be reached. On the other hand, a weak magnetic field can only push out to the bottom of the Corbet gap in MSBPs, whereas a weak magnetic field can barely push out to the propeller line in HMXBPs (the various luminosity thresholds are shown schematically in Fig. 1). MSBPs are the key to understanding binary pulsar evolution because those MSBPs with weak magnetic fields ( $B \ll 10^8 \text{ G}$ ) should behave like HMXBPs with  $B \sim 1 \text{ TG}$ , with their magnetospheres pushing out barely to the bottom of the Corbet gap. Thus, two diametrically opposite magnetospheric scales drive evolution to the same faint luminosity threshold, the bottom of the Corbet (1996) gap.

A strong magnetic field is expected to result in flaring activity originating from the bottom of the Corbet gap and from the propeller line, but not from the light cylinder in MSBPs where mass inflow is especially weak and cannot compete against the strong magnetospheric pressure. In HMXBPs, an absence of flares (a flat quiescent state) indicates that the underlying pulsars reside on the propeller line and have weak magnetic fields that are unable to play a tug of war against inflowing matter from the accretion disk (e.g., M82 X-2). We also find that ULX neutron-star sources such as M82 X-2 are true pretenders, exhibiting apparently enormous isotropic fluxes but appearing as mediocre emitters with

weak magnetic fields when their emissions are assumed to be beamed toward the direction of the observer (see also Christodoulou et al. 2017a). Such mediocre emitters with  $B \approx 0.3\text{--}0.4\text{ TG}$  have never been observed below their propeller lines (Section 3.8).

Our results for each individual pulsar have been summarized in Table 1. In this table, the reader can follow the directional arrows in order to also follow, quite easily, the flow of our calculations. As a concise comparison of our results, the main highlights from Table 1 are as follows:

(1) *Two very similar, possibly twin, short spin-period HMXBPs.*

*4U 0115+63* — This 3.61 s HMXBP is seen to cross below the propeller line and then it drops abruptly down to the bottom of the Corbet gap (Tsygankov et al. 2016a; Wijnands & Degenaar 2016), where it exhibits flaring activity indicative of a strong magnetic field ( $B = 1.3\text{ TG}$ ). The magnetic field is known independently from two cyclotron absorption lines in the spectrum. The two luminosity thresholds can be easily identified: first  $L_{\text{gap}}$  is set to  $4.5 \times 10^{33}\text{ erg s}^{-1}$  and this leads to  $L_{\text{prop}} = 1.8 \times 10^{36}\text{ erg s}^{-1}$ .

*V 0332+53* — This 4.376 s HMXBP shows very similar evolution to 4U 0115+63 (Tsygankov et al. 2016a; Wijnands & Degenaar 2016). Here, the known value of  $B = 3.2\text{ TG}$  dictates that  $L_{\text{gap}} = 1.5 \times 10^{34}\text{ erg s}^{-1}$  and  $L_{\text{prop}} = 6.7 \times 10^{36}\text{ erg s}^{-1}$ . But only one cyclotron line has been detected in the spectrum and we treated it as the fundamental. In the event that this line turns out to be the first harmonic, the luminosity thresholds would decrease by a factor of 4 and  $B$  would decrease by a factor of 2, making V 0332+53 a staunch twin of 4U 0115+63.

(2) *Two similar long spin-period HMXBPs operating well above their propeller lines.*

*AX J0049.4–7323* — This 750 s pulsar has exhibited intense variability over the past 17 years (Ducci et al. 2018), but this occurs well above the propeller line, where  $L_{\text{prop}} = 3.5 \times 10^{31}\text{ erg s}^{-1}$  for  $B = 3\text{ TG}$ . The tug of war for such a strong magnetic field against changes in  $\dot{M}$  at the inner edge of the accretion disk is certainly the reason for the observed variability.

*1A 0535+262* — This 103.3 s pulsar has also exhibited variability at a low level of  $\geq 1.3 \times 10^{34}\text{ erg s}^{-1}$  (Doroshenko et al. 2014). Its magnetic field is known to be strong from two cyclotron lines in the spectrum ( $B = 5\text{ TG}$ ). This implies that  $L_{\text{prop}} = 1.0 \times$

$10^{34}\text{ erg s}^{-1}$ , thus the flares originate above the propeller line, making the faint states of 1A 0535+262 quite similar to those of AX J0049.4–7323. Such strong variability in other long-period HMXBPs (see, e.g., footnote 1 concerning EXO 2030+375) should be indicative of strong pulsar magnetic fields.

(3) *Two MSBPs differing only in the magnitudes of their magnetic fields.*

*Aquila X-1* — This 1.8 ms pulsar exhibits all three luminosity thresholds (Campana et al. 1998; Ootes et al. 2018), which imply a strong magnetic field for its class. In cases such as this, we determine unambiguously the luminosity at the light cylinder and then we calculate the other two thresholds and the magnetic field. For Aquila X-1, we adopt  $L_{\text{lc}} = 1.0 \times 10^{33}\text{ erg s}^{-1}$  leading to  $B = 8.4 \times 10^7\text{ G}$ . Such a strong magnetic field does not allow for flaring at the light-cylinder radius because the pressure of the inflowing matter is too weak to push against the strong magnetospheric pressure.

*SAX J1808.4–3658* — In contrast to Aquila X-1, this 2.5 ms pulsar did not fade below the bottom of the Corbet gap past its two major outbursts in 2005 and 2015 (Campana et al. 2008; Sanna et al. 2017). This is an indication that its magnetic field is weak for its class, and this is the only important difference as compared to Aquila X-1. Consistent with this difference between MSBPs, we find for SAX J1808.4–3658 that  $L_{\text{gap}} = 2 \times 10^{32}\text{ erg s}^{-1}$  leading to  $B = 5 \times 10^6\text{ G}$ . Such a weak magnetic field is incapable of driving the magnetosphere toward the location of the light cylinder; nevertheless, it is expected to produce flares that crisscross the Corbet gap (which has a small extent since  $L_{\text{prop}} = 3L_{\text{gap}}$ ), as is indeed observed. Conversely, MSBPs whose light curves do not descend to the light-cylinder threshold are expected to have weak magnetic fields and exhibit flares whose X-ray luminosities fall between the other two fundamental thresholds.

(4) *A ULX pulsar with only two luminosity states and no flaring activity.*

*M82 X-2* — In 17 years of observations (Tsygankov et al. 2016b; Brightman et al. 2016), this 1.37 s ULX pulsar shows no flaring activity in its low state which however exhibits an enormous luminosity ( $L_{\text{min}} = 1.7 \times 10^{38}\text{ erg s}^{-1} \approx L_{\text{Edd}}$ ). This low state cannot be associated with the gap threshold: such an identification would lead to an unphysical magnetic field and an enormous propeller-line luminosity that the

source has never reached in its history. We identified the low state with the propeller line and we also assumed that the emission is beamed toward the observer, in which case the anisotropic propeller-line luminosity is  $L_{\text{prop}} = 1.6 \times 10^{36} \text{ erg s}^{-1}$  leading to a modest value of  $B = 0.41 \text{ TG}$ . Thus, under the assumption of anisotropic emission that does not exceed  $L_{\text{Edd}}$  during the most powerful outbursts, this ULX source appears to be quite a common pulsar that is similar to many Magellanic HMXBPs with modest magnetic fields (Christodoulou et al. 2016). More importantly, irrespective of whether the emission is beamed or isotropic, the jump factor of M82 X-2 above the lowest Magellanic propeller line is only  $J = 2$  (Christodoulou et al. 2018), which indicates the presence of a weak magnetic field, comparable to that of the lowest Magellanic propeller value of  $0.29 \text{ TG}$ .

**Acknowledgements** We are very much obliged to a referee whose comments led to a significantly clearer presentation of our results. DMC and SGTL were supported by NASA grant NNX14-AF77G. DK was supported by a NASA ADAP grant.

## References

- Bachetti, M., Harrison, F. A., Walton, D. J., et al. 2014, *Nature*, 514, 202
- Bildsten, L., Chakrabarty, D., Chiu, J., et al. 1997, *ApJS*, 113, 367
- Brightman, M., Harrison, F., Walton, D. J., et al. 2016, *ApJ*, 816, 60
- Caballero, I., Pottschmidt, K., Marcu, D. M., et al. 2013, *ApJ*, 764, L23
- Campana, S., Stella, L., Mereghetti, S., & Colpi, M. 1995, *A&A*, 297, 385
- Campana, S. 1997, *A&A*, 320, 840
- Campana, S., Stella, L., Mereghetti, S., et al. 1998, *ApJ*, 499, L65
- Campana, S., Stella, L., & Kennea, J. A. 2008, *ApJ*, 684, L99
- Campana, S., & Di Salvo, T. 2018, “NewCompStar” European COST Action MP1304, in press
- Chakrabarty, D., Bildsten, L., Finger, M. H., et al. 1997, *ApJ*, 481, L101
- Christodoulou, D. M., Laycock, S. G. T., Yang, J., & Fingerman, S. 2016, *ApJ*, 829, 30
- Christodoulou, D. M., Laycock, S. G. T., Kazanas, D., Cappallo, R., & Contopoulos, I. 2017a, *RAA (Research in Astronomy and Astrophysics)*, 17, 63
- Christodoulou, D. M., Laycock, S. G. T., Yang, J., & Fingerman, S. 2017b, *RAA (Research in Astronomy and Astrophysics)* 17, 59
- Christodoulou, D. M., Laycock, S. G. T., & Kazanas, D., *RAA (Research in Astronomy and Astrophysics)*, 2018, 18, 128
- Corbet, R. H. D. 1996, *ApJ*, 457, L31
- Dall’Osso, S., Perna, R., Papitto, A., Bozzo, E., & Stella, L. 2016, *MNRAS*, 457, 3076
- Doroshenko, V., Santangelo, A., Doroshenko, R., et al. 2014, *A&A*, 561, A96
- Ducci, L., Romano, P., Malacaria, C., et al. 2018, *MNRAS*, A&A, in press
- Earnshaw, H. P., Roberts, T. P., & Sathyaprakash, R. 2018, *MNRAS*, 476, 4272
- Frank, J., King, A., & Raine, D. J. 2002, *Accretion Power in Astrophysics: Third Edition* (Cambridge: Cambridge University Press), 398
- Fürst, F., Kretschmar, P., Kajava, J. J. E., et al. 2017, *A&A*, 606, A89
- Ghosh, P., & Lamb, F. K. 1979, *ApJ*, 234, 296
- Ghosh, P., Lamb, F. K., & Pethick, C. J. 1977, *ApJ*, 217, 578
- Hartman, J. M., Patruno, A., Chakrabarty, D., et al. 2008, *ApJ*, 675, 1468
- Illarionov, A. F., & Sunyaev, R. A. 1975, *A&A*, 39, 185
- Lorimer, D. R. 2008, *Living Reviews in Relativity*, 11, 8
- Makishima, K., Mihara, T., Ishida, M., et al. 1990, *ApJ*, 365, L59
- Naik, S., Dotani, T., Terada, Y., et al. 2008, *ApJ*, 672, 516
- Ootes, L. S., Wijnands, R., Page, D., & Degenaar, N. 2018, *MNRAS*, 477, 2900
- Papitto, A., & Torres, D. F. 2015, *ApJ*, 807, 33
- Papitto, A., Torres, D. F., Rea, N., & Tauris, T. M. 2014, *A&A*, 566, A64
- Patruno, A., Watts, A., Klein Wolt, M., Wijnands, R., & van der Klis, M. 2009, *ApJ*, 707, 1296
- Phinney, E. S., & Kulkarni, S. R. 1994, *ARA&A*, 32, 591
- Reig, P. 2011, *Ap&SS*, 332, 1
- Rouco Escorial, A., Bak Nielsen, A. S., Wijnands, R., et al. 2017, *MNRAS*, 472, 1802
- Sanna, A., Di Salvo, T., Burderi, L., et al. 2017, *MNRAS*, 471, 463
- Spruit, H. C., & Taam, R. E. 1993, *ApJ*, 402, 593
- Stella, L., White, N. E., & Rosner, R. 1986, *ApJ*, 308, 669
- Tsygankov, S. S., Lutovinov, A. A., Doroshenko, V., et al. 2016a, *A&A*, 593, A16
- Tsygankov, S. S., Mushtukov, A. A., Suleimanov, V. F., & Poutanen, J. 2016b, *MNRAS*, 457, 1101
- Vybornov, V., Doroshenko, V., Staubert, R., & Santangelo, A. 2018, *A&A*, 610, A88
- Wang, Y.-M. 1987, *A&A*, 183, 257
- Wang, Y.-M. 1995, *ApJ*, 449, L153
- Wang, Y.-M. 1996, *ApJ*, 465, L111
- White, N. E., Swank, J. H., & Holt, S. S. 1983, *ApJ*, 270, 711
- Wijnands, R., & Degenaar, N. 2016, *MNRAS*, 463, L46